 DOI: 10.1002/masy.200751001

Polymer Networks in Research and Application

Walther Burchard

Summary: The present review presents an attempt to trace common aspects in the research on networks of very different origin, directed to industrial or biochemical applications. One major feature is the preparation of thermal, pH or ionic sensitive core/shell structures. These elements proved to be significant in the field of reinforcement of rubbery materials as well as for suitable design of scaffolds for tissue engineering. Striking properties are reveal with examples of thermo- and magneto-sensitive core/shell microgels. Two other instances of oscillating systems are discussed. One was directed to the development of nano-scaled motors, the other to broadcasting biochemical relevant signals via oscillating Ca^{++} and H^{+} ions in vesicle/cytosol systems. Finally problems and progress in scaffold preparation are discussed.

Keywords: networks; microgels

Introduction

Research in the past 30 years has dealt, predominantly, with covalent or *permanent networks and gels*, assuming essentially homogeneous crosslinking density. *Aggregation* has been studied mostly with polysaccharides.[1,2] General principles for thermoreversible gelation was shown on the basis of multiple helix formation or cooperative side-by-side association. With the exception of a few groups,[1,3] this principle was largely disregarded by synthetic polymers chemist. *Liquid crystalline networks* from lyotropic side-chain or main-chain polymers were discussed only sporadically focussing mostly on the orientation of chains and the order parameters. Only recently has interest in research grown by rediscovering the potentiality of clays albeit mainly under the auspices of network reinforcement. Crosslinked liquid crystalline networks are still studied in other groups but predominantly within the theme of common liquid crystalline properties. Flory in 1974 mentioned as a fourth type of networks *particulate, disordered structures*, and was probably thinking of proteins e.g. the fibrin network on blood clotting, and antigen-antibody reactions. He certainly had no clear imagination how vividly the research in this field would develop to be one of the most attractive subjects. On the whole Flory's classification in 1974 comprises the main features of polymer networks. A list of reviews and books is given in the references.

In view of this general classification we may wonder whether in our present research we are merely filling gaps in an essentially well understood field, or something new is going on. I looked at some subjects which were outside my own experience and was surprised by the vital creativity in fields which I had not followed so carefully in the past. The purpose of the present contribution is an attempt to trace a common line that would link very different topics in recent research. My rather personally motivated selection was made from (i) Reinforcement of Networks, (ii) Processing of Networks, (iii) Responsive Core/Shell Microgels, (iv) Motile Systems and (v) Mesoscopic Systems.

Reinforcement of Networks

Rubber reinforcement by fillers is almost historic. The first theoretical approach to

Institute of Macromolecular Chemistry, Albert-Ludwig-University of Freiburg, 79104 Freiburg, Germany
E-mail: walther.burchard@makro.uni-freiburg.de

describe this phenomenon was made by Smallwood in 1944[4] who applied the same approach as was used by Einstein for the derivation of the increase in viscosity by the volume of hard spheres. This hydrodynamic approach is known as the Einstein-Smallwood[4a,b] equation. The reinforcement f can be expressed by the Young's elastic module E or the shear modulus G

$$\frac{E}{E_0} \equiv f = 1 + 2.5\varphi \approx \frac{2.5\phi}{1-2\phi} \quad (1)$$

where for incompressible systems $E = 3G$. E_0 refers to the unfilled network and ϕ is the volume fraction of spheres in the network. Figure 1 elucidates the effect of a filler. The Padé approximation (last term in Equation 1) was later added to take into account interactions between clusters of spheres.

The equation still remains unsatisfactory. Such filler material occurs mostly as clusters, and such aggregates do not behave like hard spheres. Furthermore the filler particles will have an elastic modulus smaller than that of hard spheres. The Smallwood theory was later generalized to include aggregated fillers of finite shear moduli and led to a general equation of [5]

$$\frac{E}{E_0} = 1 + \frac{[\mu]\phi}{1 - 2/5[\mu]\phi} \quad (2)$$

with an intrinsic modulus

$$[\mu] = \frac{1}{\phi}\left[\frac{E - E_0}{E_0}\right] at\ \phi = 0 \quad (3)$$

The intrinsic modulus can be obtained experimentally by extrapolation to zero filler concentration, but for special cases it also could be calculated by theory. Jones et al.[6] obtained for uniform fillers

$$[\mu] = 5\frac{1-\overline{\mu}}{2-3\overline{\mu}}; \quad \overline{\mu} = \frac{E_m}{E_{filler}} \quad (4)$$

where E_m and E_{filler} are the elastic moduli of matrix and filler.

Core/Shell structure of fillers in a polymer matrix

There have been early conjectures that the filler particles may be surrounded by a glassy shell (see Figure 2).

This supposition was confirmed in careful studies by Beriot et al.[7,8] The authors measured the relaxation times by NMR and found two well separated modes which could be assigned to the mobility of chains on the matrix and of layers around the fillers. From the amplitudes of the two relaxations and the filler concentration they estimated the thickness of the layer. The shell thickness, varied with temperature, from 1.5 to 2.8 nm in the range 50–100 °C above the matrix glass temperature. A radial gradient in the elastic modulus was suggested.[8]

Stimulated by these recent findings Huber et al.[9] set up a generalized theory that takes account of the core/shell structure and partial interpenetration of aggregated filler particles. The theory is not trivial, and only the final results will be mentioned here. In a first attempt scaling arguments were applied by assuming diffu-

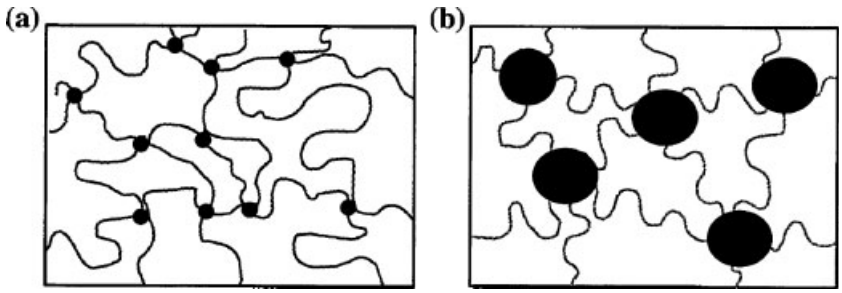

Figure 1.
Illustration of reinforcement by hard sphere fillers. The filler particles cannot be deformed, and an overstretching of network chains occurs compared to the unfilled network chains. (a): unfilled network, (b): filled network.

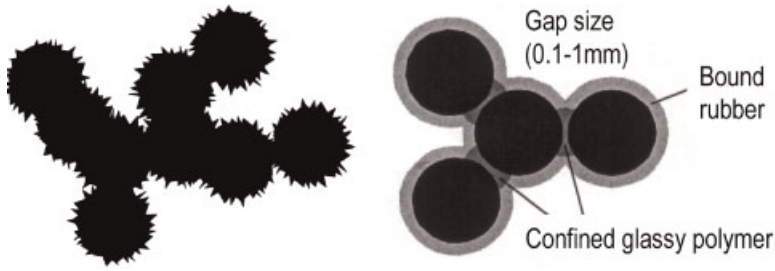

Figure 2.
Aggregates of primary filler particles (left) and a schematic picture of a glassy shell around the filler aggregate (right).[9] (By permission of ASC)

sion controlled cluster-cluster aggregation. The theory gave exponents for the power law behaviour of the reinforcement as a function of the volume fraction ϕ but not of the magnitude. In a second approach the authors confined themselves to non-aggregated core/shell particles. Figure 3 shows the result of reinforcement of hard spheres, coated by a shell of constant modulus $E_{shell} > E_m$ as a function of ϕ, for a set of increasing shell thickness. A remarkable additional reinforcement by the shell was obtained.

An interesting feature of this study emerged when the authors calculated the effect of a soft core surrounded by a shell of higher modulus than the matrix. Here, of course, the rubber becomes softer with decreasing shell thickness. The limiting case of hollow spheres (i.e. $E_{core} \approx 0$) corresponding to rubbers of the Swiss cheese type is shown in Figure 4. This type of filler is of special relevance in bioengineering as will be demonstrated in the last part of this contribution.

Neutron scattering from a filled model network

The elastic modulus of rubbery materials is mostly measured by stress-strain/rheological techniques. Colleagues from the German Federal Research Centre in Jülich[10] were interested in a method that would allow them to measure the reinforcement by scattering techniques. The idea was, if an unfilled and a filled rubber are stretched to the same extent, the network chains in the filled matrix will be stretched more,

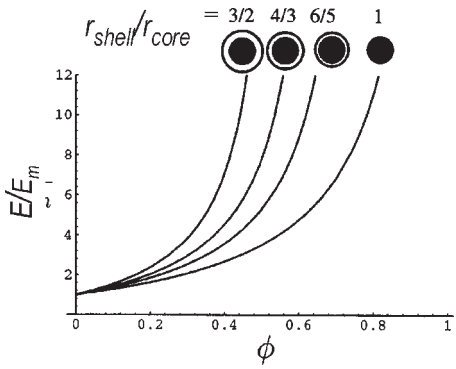

Figure 3.
Reinforcement by hard sphere fillers with shells of different thickness.

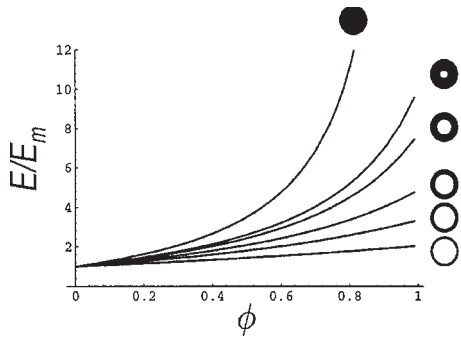

Figure 4.
Softening by hollow core fillers of different shell thickness.[9](By permission of ACS)

because the hard filler does not deform. Figure 1b shows this effect. For incompressible systems the reinforcement factor $f = E/E_m$ can be expressed by this overstrain.

$$\lambda_{filled} - 1 = f(\lambda - 1) \tag{5}$$

where λ and λ_{filled} correspond to the strains of chains in the unfilled and filled systems.

The authors prepared a model network that was based on a tri-block PI-**PS**-PI copolymer (PI: polyisoprene, PS: polystyrene) of composition 41/18/41. At this composition the PS blocks collapse and become regularly dispersed in the flexible PI matrix. The scattering from the PS spheres could be suppressed in small angle neutron scattering (SANS) by mixing hydrogenated PI(H) with deuterated PI(D) monomers in an appropriate ratio and polymerizing the two PI wings of the tri-block with this mixture. Furthermore, monodisperse PI(H) and PI(D) chains of about the same lengths were prepared separately. Two different concentrations of the tri-block copolymer and the two PI chains, in the ratio of the monomers in the tri-block copolymer, were mixed in THF. Dicumylperoxide was added as crosslinker and the system was cured at 163 °C under an argon atmosphere in a mould. After evaporation of THF three types of measurement were carried out. (i) X-ray scattering at the DESY Synchrotron in Hamburg. These data represent the whole network structure.(ii) SANS measurements from the filled network at various strains (λ), and (iii) SANS measurements from the unfilled network at the same strain (λ). Only the (D)-labelled network chains are probed by SANS. The dimensions of the labelled strained chains in the filled (λ_{filled}) and unfilled (λ) networks were measured and compared. The reinforcement factor f for incompressible systems is given by Equation (5)

A theoretical expression for the particle structure factor of stretched chains in the network is needed to realize this approach. The corresponding work was done by Heinrich et al.[11] on the basis of Sam Edwards' tube model [12] and is given by the equation

$$S(q,\Lambda) = 2\int_0^1 dX \Pi(1-X) \times \exp\left\{-[(q_\mu R_g \to \lambda_\mu)^2 X - (q_\mu R_g)^2 (1 - \to \lambda_\mu^2)\frac{d_\phi^2}{2\sqrt{6}R_g^2}\left(1 - \exp(-\frac{x(2\sqrt{6}R_g^2)}{d_\phi^2}\right)\right\} \tag{6}$$

where the product runs over the coordinates $\mu = x, y, z$ and $X = s/L$ denotes a chain section s along the chain divided by the contour length L of the labelled chain. This equation looks formidable, but one recognizes that at $\lambda_\mu = 1$ (unstretched network) the second term in Equation 6 disappears and the equation reduces to the well-known Debye scattering function of linear flexible chains. This function is modified by the strain according to the second term which contains the tube diameter d_ϕ. A straight forward calculation was first made with the known strain value of the unfilled network which gave systematic deviations from the experiment. In a second step the strain was modified by multiplying this with a reinforcement factor f until a best fit of the scattering curves was achieved. Figure 5 shows the optimized result for two detector distances (small and large q).

Shear thinning, hysteresis and break down of reinforcement

The above results were obtained for small deformation. Additional conclusions were obtained when a moderate deformation was applied. A marked shear thinning and a pronounced hysteresis after pre-stretching the network were observed, which were not seen with the unfilled network. The conclusion was that under shear deformation a

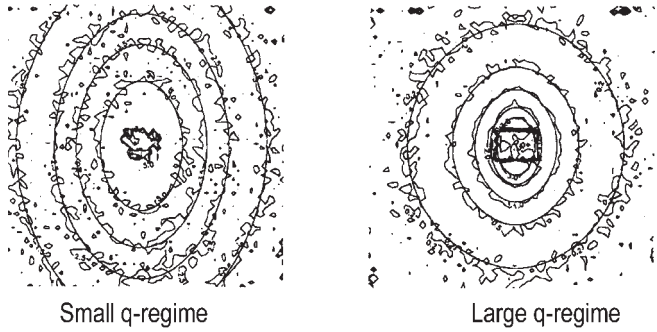

Figure 5.
Two dimensional scattering profile of SANS measurements from the PI-**PS**-PI model network the solid lines correspond to the best fit by Equation 5.[10] (By permission of ACS)

rearrangement of the aggregated clusters had taken place in the stress direction.

However this arrangement is not permanent and is partially reversible causing marked hysteresis. This effect makes a significant contribution to the rolling resistance of car tires.[13] Figure 6a presents a diagram of the rearranges filler clusters and Figure 6b shows the stress-strain behaviour for pre-stretched networks under cyclic strain. For details see [14,15].

At large stress the clusters are partially disrupted but in the relaxed state they slowly re-aggregate[16] The modulus breakdown is shown in Figure 7.

Processing of Crosslinked Materials

This topic leads into a very different field. We know of the difficulties in transferring a reacting system into a mould. This should not be performed too early but certainly before gelation or vitrification takes place. In laboratory work we have time to find the optimum conditions. But in processing the entire specimen should have the same shape and the same properties, show only small ageing effects after the process. Most important, the processing of each specimen should be performed as fast as possible. Clearly, the kinetics and the various stages of the process, (i.e. phase separation, vitrification or crystallization and sol-gel transition) have to be known as accurately as possible, before a program for the process can be set up.

One of the simplest processes is the so-called Reaction Injection Moulding (RIM) which intensely was studied by the group of John Stanford in Manchester.[17] The technique is specially appropriate for processing fairly thin specimen of complex shapes (about 3 mm thickness). The

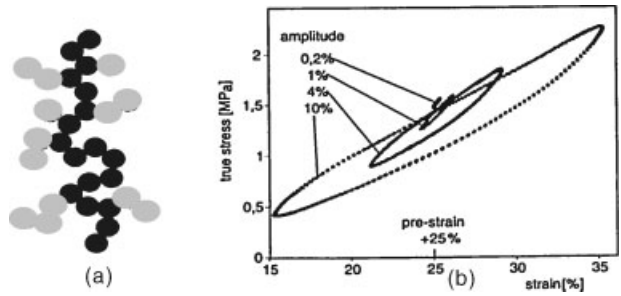

Figure 6.
(a) Filler clusters partially de-aggregate and rearrange along the stress direction: (b) Cyclic stress-strain curves of pre-stretched networks disclose hysteresis[13] (By permission of Swets & Zeitlinger)

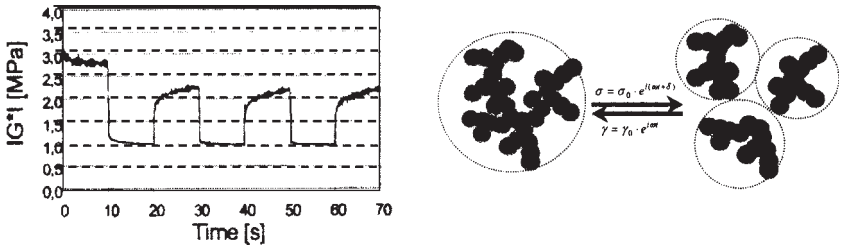

Figure 7.
Break-down and recover of the elastic modulus under large deformation (left) and corresponding clarification by diffusion controlled de-aggregation and reformation of filler-clusters (right).(By permission Huethig Verlag)

principle appears simple at first sight. In two separate vessels the reactants, e.g. a triol and a diisocyanate, are filled in the desired volume ratio and brought to a certain temperature. Then these two components are mixed in a high pressure chamber that guarantees quick and turbulent mixing. The mixture is filled into a preheated mould, but now at low pressure to prevent turbulence. After the curing reaction had led to a fixed shape the sample is ejected and left outside the mould for after-curing. A gel content of 80% or higher could be obtained. The time in the mould should last not much longer than 60 seconds.

Interest has been directed more to complex reactions. Figure 8 shows as an example two bi-functional monomers which can react with each other to give an alternating copolymer, but also with a tri-functional 3 arm star-branched component with flexible arms, which acts as a crosslinker. (See Figure 8)

The reaction in this system leads to segmented hard- and soft-block polyur-

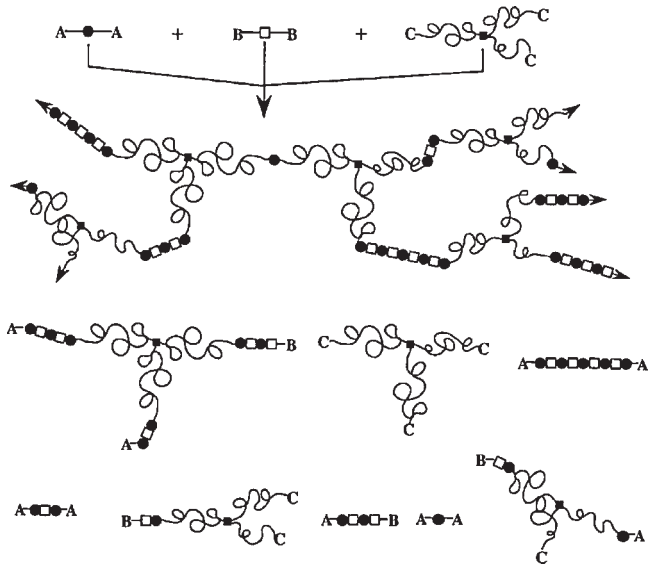

Figure 8.
Components and possible reactions in a complex RIM process. B can react with A; C can react with A; but no other reactions are possible. Block segmented structures result, often accompanied by micro-phase separation.[17] (By permission of Chaman amd Hall)

ethanes. Such structures are of need whenever the material has to sustain a certain tensile stress, still combined with elastic softness. As an example it could be used as a substitute for blood vessels where the circulation should not initiate rupture of the blood platelets with concomitant clotting of the blood.

Figure 9 demonstrates which problems can occur and how to overcome them. Since the viscosity will increase strongly shortly before the sol-gel transition occurs, the reaction mixture has to be injected in the mould after a short reaction time of in the mixing chamber. The desired gel-point is often not reached because of vitrification or crystallization. In such cases a physical network is obtained, which further reacts very slowly by diffusion control, causing undesirable ageing effects. Usually the process is even more complex, due to incompatibility between chemically different blocks which leads to microphase separation. This in turn changes the kinetics of structure formation, often in an unpredictable manner. Here computer simulations become a very important tool.

Homogeneous and Core/Shell Microgels

Microgels have many properties in common with homogeneous macrogels i.e. constant average segment density and no local domains of higher crosslinking density. At low conversion, or low crosslinker concentration, randomly branched clusters are formed in a small confined domain, e.g. latex particles. At the critical conversion, when network formation commences, some of the clusters have reached the size of the microscopic vessel. Beyond this gel-point, disproportionation occurs into a gel- (network) and a sol-fraction that can be determined by SEC, dialysis and precipitation.[18,19] Near the gel-point critical behaviour (power law dependence) is obtained. However the critical exponent in microgels deviates from that in macrogels.[20] The nano-size of the microgels made possible measurements of significant structural properties which are not accessible with macroscopic networks. Nowadays, internal or segmental motions can be studied as well as the radius of gyration and the hydrodynamic radius. In dynamic LS a time

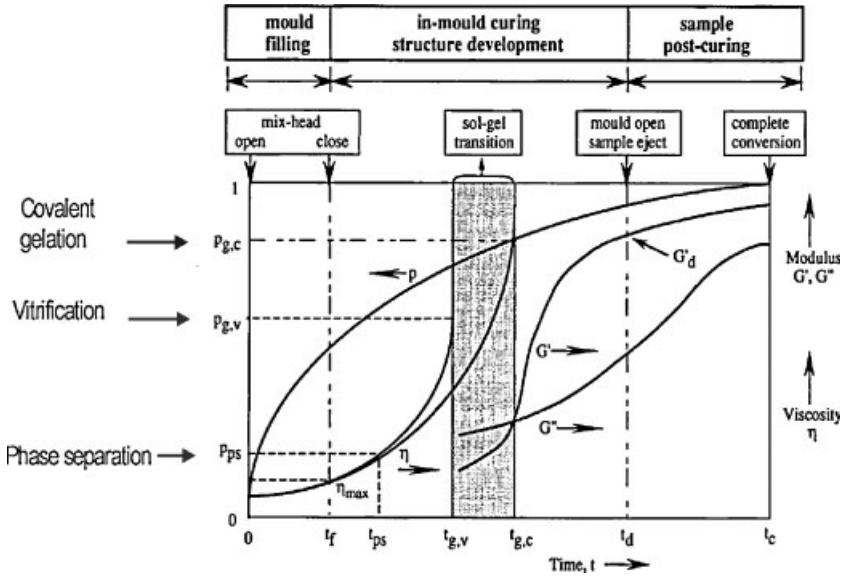

Figure 9.
Scheme of reactions in the course of reactions in a reactive injection mould.[17] (By permission Chapman & Hall)

correlation function (TCF) is measured which at short delay times decays like a single exponential. The decay constant is called the first cumulant of the TCF. The time correlation function depends on the delay time and the scattering vector $q = (4\pi n_0/\lambda_0)\sin(\theta/2)$, which is related to the scattering angle θ. It is instructive to use qR_g instead of q as variable, where R_g is the radius of gyration. For instance, at $qR_g > 4$ distances are probed by light scattering which are four times smaller than the radius of gyration. In other words, structure and mobility of short chain segments are probed.

For linear chains in solvent, hydrodynamic interactions occur between the chain segments and the overall behaviour can be described by the well-known Zimm model. According to this model the first cumulant increases proportional to q^3 at large qR_g, so that a constant value should be obtained when the first cumulant is divided by q^3. This, indeed, was found with a number of chemically different flexible linear chains. The dotted line in Figure 10 represents the findings from PS and PI chains. For branched chains a shift to smaller values is observed, and this shift becomes more pronounced with the branching density. The effect is especially marked with microgels.[21] These findings stand in contrast to the common opinion that chains between crosslinks behave like flexible Gaussian chains. In a range from large to rather short distances in the particle, the dynamics displays the behaviour of hard spheres. Only at even shorter distances does internal mobility become noticeable. Evidently the slow internal motions are suppressed quite efficiently by branching or cross-linking. It still remains unclear whether or not the remaining motions follow the Zimm form of relaxations, and theories on this effect are still missing.

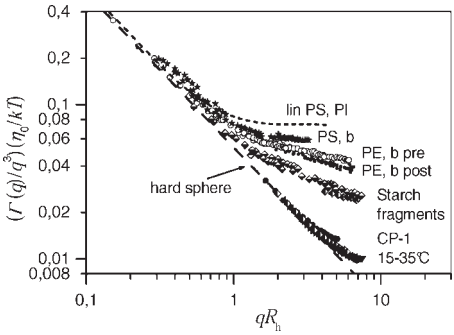

Figure 10.
Plot of the reduced first cumulant as a function of qR_h of dynamic light scattering data from a thermosensitive microgel and some branched macromolecules in solution.[21] (By permission of ACS)

Core/Shell Microgels[22]

With these structures controlled heterogeneity is introduced to the particles. Countless different preparations have been published.[22] I made a selection of two examples. Richtering et al.[23] used two thermo-responsive polymers, the well known poly(N-iso**p**ropylacrylamide), (poly (NI**P**AM)) and the other poly(N-iso**p**ropyl**m**ethylacrylamide), (poly (NI**PM**AM)). The lower critical solution temperatures (LCSTs) occur at about 32 °C and 45 °C respectively. Two complementary core/shell microgels were prepared (i) poly (NI**PM**AM)-core/poly(NI**P**AM)-shell and the inverse (ii) poly(NI**P**AM)core/poly (**NIPM**AM)-shell microgel. The effect of shell thickness and crosslinking density of the shell on the swelling behaviour was studied in the temperature range from 25–50 °C.

Figure 11 shows the well-known change with temperature of the hydrodynamic radius of the poly(NI**P**AM) core and that of the corresponding poly(NI**PM**AM)/poly(NI**P**AM) core/shell microgels. Two striking facts were observed. (i) The core/shell particle nicely displays two inflection points corresponding to the LCSTs of the two polymers, slightly shifted to lower temperatures compared to that of the isolated core. (ii) At intermediate temperatures of 34–42 °C the core/shell microgel has lower dimensions than even the core alone. Evidently the collapse of the shell prevents swelling of the core. The findings were supported by combined LS/SANS

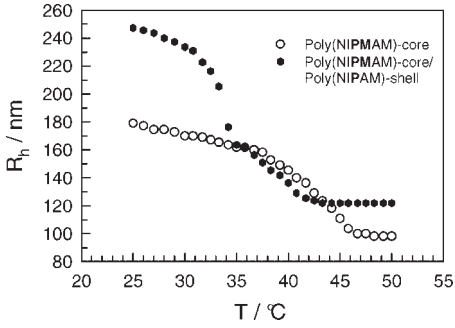

Figure 11.
Temperature dependence of the hydrodynamic radius of a poly(NIPAM) microgel of the same size as the core in the core/shell Poly(NIPMAM)/poly(NIPAM) microgel.[22a] Note, the LCST of the core is 45 °C that of the shell 32 °C; in the intermediate temperature range the shell is in the collapsed state but not the core.[23a] (By permission of ACS)

measurements[23b] at selected temperatures of 25, 39, and 50 °C corresponding to fully swollen, intermediate, and collapsed states. Similarly the swelling becomes more inhibited either with increasing shell thickness or by increasing the crosslinking density of the shell.[23a,b]

These effects are essentially as expected. More interesting are results from the opposite composition, i.e. the poly(NIPAM) as core. The effects of shell thickness and crosslinking density of the shell were studied keeping the core constant in size and crosslinking density.[23c] Figure 12a,b show the swelling behaviour for shells of three crosslinking densities.

At a first sight everything looks as expected, shell thickness and increasing cross linking density inhibit the swelling. However, a quantitative analysis disclosed an unexpected effect. Assuming additivity from both components the swelling can be calculated from the swelling of the one component microgels. Considerably larger hydrodynamic radii were measured than calculated. This is shown in Figure 12a. Obviously the less hydrophobic poly(NIPMAM) in the shell forces the poly(NIPAM) core to become overstretched. In other words a synergistic swelling effect occurs. The inset Figure 12b gives the overstretching factors as a function of crosslinking density. Similar synergistic swelling was observed earlier[24] with star-microgels, i.e. a poly(methylmethacrylate) (PMMA) core covered by short poly(styrene) (PS) chains in 10 different organic solvents. with a maximum overstretching factor of around 2.We assigned the effect to incompatibility of PS with PMMA and the induced segregation.

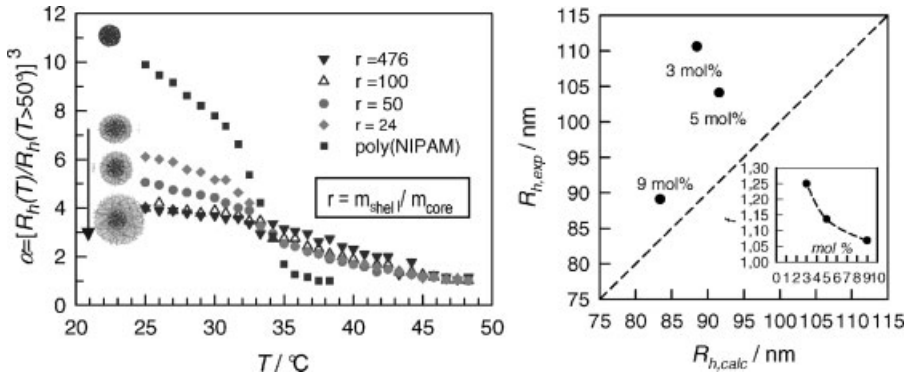

Figure 12.
(a)Swelling ratio of poly(NIPAM)-core/polyNIPMAM)-shell for shells of the same thickness but different crosslinking density (indicated by % crosslinker used).The swelling was calculated from the cube of the hydrodynamic radius at a certain temperature compared to that at 50°, the collapsed states for both polymers. (b) Measured hydrodynamic radii as a function of calculated radii assuming additivity of both components. The inset shows the overstretching factor.[23c] (By permission of ACS)

Networks with embedded core/shell super-paramagnetic particles.[25,26]

The second type of core/shell structures were prepared by Annette M. Schmidt[25,26] from the University of Düsseldorf. She succeeded in grafting special initiators onto the surface of precipitated Fe_2O_3 particles of about 12 nm diameter. With this size the ferrite displays super-paramagnetic behaviour. With the attached initiators a shell of poly(methoxyethyl-methacrylate) (PMEA) could be polymerized by the ATRP technique, or poly(ε-caprolactone) (PCL) by ring opening procedure. Scheme 1 (top) shows the reactions and Scheme 1 (bottom) the reactions of three different polymers attached to the particle surface.[25a,b]

The shell of polymer chains shields the magnetic core and prevents coagulation of the magnetic particles. Annette Schmidt had medical applications in mind, for instance to stabilize magnetic fluids so that, when injected into tumour cells, they could be heated by friction in an alternating magnetic field, to allow hyperthermic treatment.

More exciting was the embedding of the core/shell microgel into a polymer network. Amorphous poly(ε-caprolactone) forms crystal domains on stretching. The melting temperature of crystals from long chains is with about 70 °C much too high for body temperature. However, the melting temperature is drastically decreased for oligo-PCL. These core/shell particles of short shell chains w ere mixed with bifunctional methacrylate macromonomers, prepared on the basis of oligo PCL chains with a short butylacrylamide section, yielding a melting temperature of 42 °C. After adding AIBN, crosslinking was performed at 70 °C, well above the glass and melting tempera-

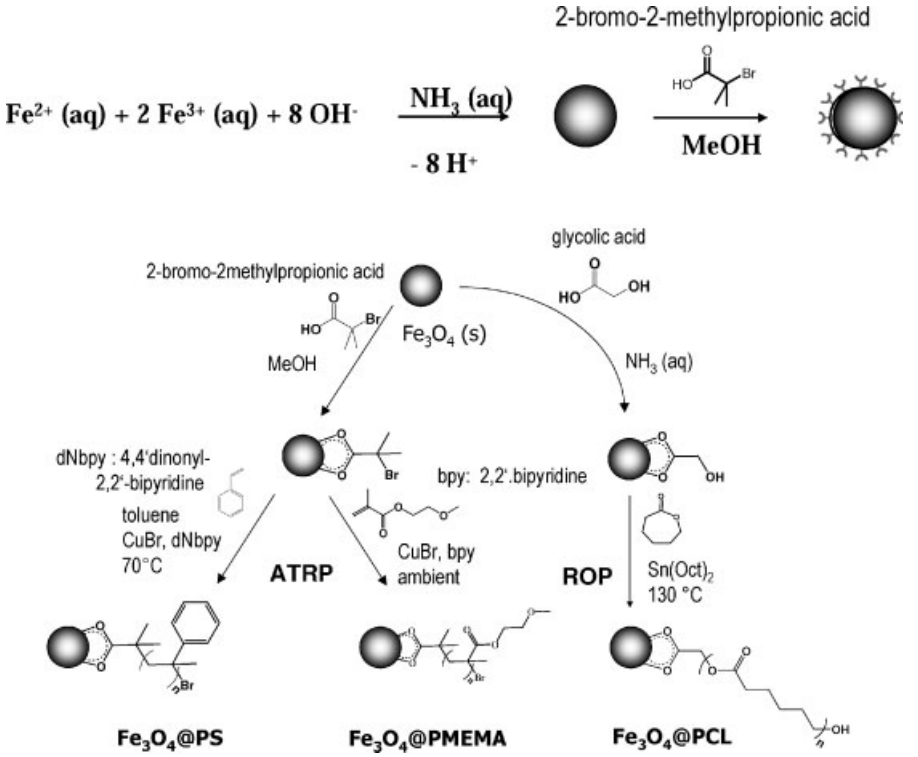

Scheme 1.

(above)**:** Scheme of reaction to prepare hyper-paramagnetic particles and the attachment of chains by ATRP polymerization, (below) reaction schemes for three core/shell particles.[25a,c], (Personal contribution by A.M. Schmidt)

tures of the network-chains. A strip of network was stretched and slowly cooled to room temperature, keeping the strain constant, whereupon crystallization occurred. After quenching the partial crystallinity this state could be kept stable at room temperature. Then the sample was brought into a high frequency alternating magnetic field which caused heat development within less than one second. At 42 °C the small crystals melted, and the sample should return to the original equilibrium molten state. Scheme 2 shows the principle.[26]

Photographs from experiments with a thin strip showed relaxation to nearly the original shape within 10–20 seconds. The effect was even clearer with a small tube that was coiled up to form a helix. The paper did not comment on possible application, but the use of a micro-tube gives rise to some speculation, for instance to use the system as stents in clogged heart-coronary arteries.

A short comment was made that with the embedding of the paramagnetic core/organic shell nano-particles noticeable reinforcement was observed. With this comment the work by Richtering and Schmidt made clear the relevance of these studies also for the reinforcement in rubbers. Apparently the swelling capability of core/shell particles is related to the elastic modulus of these nano-particles.

Motile Systems

Motor-like periodic expansion/shrinking of a model network

Fairly early in the history of polymer science pronounced changes in swelling of polyelectrolyte gels was observed when the pH or the ionic strength of the aqueous medium was varied. This aroused the question whether use could be made of this property to design artificial muscles. For instance, a strip of cross-linked poly(acrylic acid) could be immersed in a weakly acidic aqueous medium. On increasing the pH towards 14 and returning to the acid range, a pronounced swelling/deswelling will be obtained which could be used to do mechanical work. Indeed, this effect is obtained but with a very slow diffusion limited rate. A design of a system had to be developed in which the transport distances are microscopically short. The desired macroscopic work could be attained by several coupled microscopic elements, but pH would have to be controlled externally by suitable feeding programs of acids and bases. This possibility is

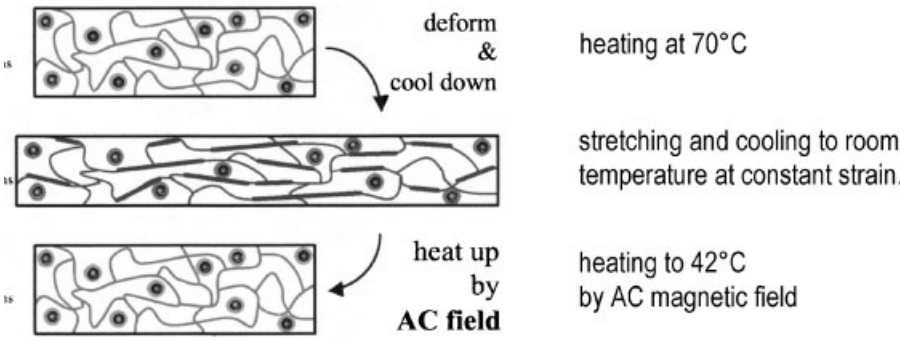

Scheme 2.
Electromagnetic activation of shape-memory networks containing magnetic nano particles. Components: Fe_3O_4/PCL core/shell particles; BA-PCL-dimethacrylate macromonomer (cross-linker), oligoPCL, AIBN (initiator). Procedure: After cross-linking the filled network was heated to 70 °C and stretched. The system was slowly cooled to room temperature keeping it in the stretched position whereupon crystallization of the network chains occurs. Application of a 300 kHz magnetic resonator at 5 kW raised the temperature to 42 °C and caused return of the network shape to its unstretched form.[26] (By permission of Wiley & Sons)

far from that of an engine in which fuel is put into a tank, and the drive is made by the engine itself. Clearly, besides the request of coupled microelements the system must comprise repetition of a working cycle without the application of an external steering program.

Anthony Ryan and co-workers[27] solved the chemical requirements with a special model network. They prepared a PMMA-**PMAA**-PMMA tri-block copolymer, by first polymerizing the corresponding tri-block copolymer with PtBuMA as the middle block, which later was transformed to the polyacrylic acid (PMAA) by saponifying the tertiary butyl esters. The block-copolymer was dissolved in a solvent mixture of acetone/methanol (85/15) in which both block types were soluble. A high concentration was chosen to restrict undesired cyclisation. By slowly evaporating the solvent, acetone is removed first followed by phase separation of the PMMA blocks, while the central PMAA block remained swollen until all methanol was removed. A small strip of this material was immersed in water. The PMMA blocks remained in the collapsed state and formed the junction domains, but the PMAA blocks could swell. Thus with the small strip and the pH sensitive nano-sized blocks the first condition of short distances was fulfilled. To get a motor running with a chemical fluid, an oscillating chemical reaction had to be found. Ryan remembered the well known oscillating Landoldt reaction[27,28] which was applied with the following composition. 0.16 M $KBrO_2$, 0.066 M $K_4Fe(CN)_3$; 0.3 M Na_2SO_4, 0.04 M H_2SO_4. The reaction starts at pH 6.6 and runs towards the acidic range. At pH 3.3 a transitional time interval of fairly slow change to pH 4 took place but then abruptly flipped to a fast reaction back to the starting pH 6.6. A new cycle started. One cycle took about 20 minutes. To keep constant conditions the team applied continuous flow through the chamber that contained the physical gel. Swelling and shrinking of the strip was measured macroscopically by a CCD camera and simultaneously recorded microscopically by SANS diffraction. The ordered morphology of the network gave rise to a diffraction peak that corresponded to the distance between the PMMA blocks. The swelling of the nano PMAA blocks increased the distances among the PMMA blocks and caused shift of the diffraction peak towards smaller *q*- values.

Scheme 3 shows the principle and Figure 13 shows the relative expansion observed by SANS and video camera. Complete in-phase behaviour indicated affine network behaviour.

Oscillating $Ca^{++}/K^{+}/H^{+}$ ion fluctuations in polyelectrolyte networks of transport vesicles[29]

Oscillatory reactions are rare in chemistry but are important in biochemical reactions and also may become relevant in nano-scale chemical engineering. An essential condition for such reaction[28] is the presence of *bistability* a designation that is equivalent to undercooling in equilibrium thermodynamics. In short the initial stage, far away

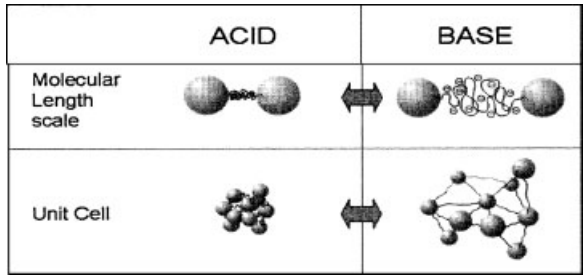

Scheme 3.
Oscillating breathing of the domains in the nano scale and of the macroscopic network strip under influence of a Landoldt oscillator [27] (By permission of Taylor and Francis)

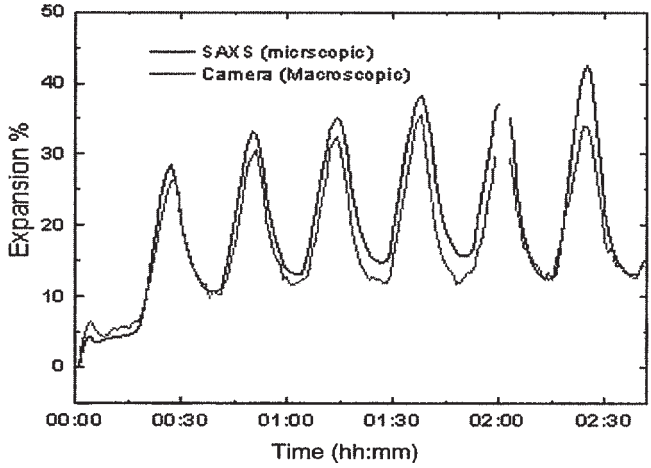

Figure 13.
Oscillation pH of the Landolt reactor (left) and the relative changes observed micro- and macroscopically, (right).[27](By permission of Taylor & Francis)

from equilibrium, has to be a smooth and stable reaction. At a critical conversion the system suddenly switches to a back-reaction that again remains stable up to another critical conversion when the reaction turns to the forward reaction etc. Recently Pedro Verdugo[29] discovered such oscillating fluctuations of Ca^{++} and H^+ ions concentrations in vesicles of mouse mast cells with two specific channels in the membrane: one inositol triphosphate, shortly named $InsP_3$-R, which allows controlled transport of Ca^{++} from the vesicle into the cytosol, the other, nearby in the membrane, an apamin-sensitive Ca^{++}-sensitive K^+ channel (ASK_{Ca}) for K^+ flowing form the cytosol *into* the lumen of the vesicle. The Ca^{++} concentration in the cytosol is normally very low. Under this condition the K^+ importing ASK_{Ca} channel is closed. When the Ca^{++} concentration in the cytosol has increased beyond a certain limit the $InsP_3$ channel is closed. Simultaneously the ASK_{Ca} channel opens and allows a flux of K^+ into the vesicle lumen. In mast cells the vesicles transport histamine that is bound to a network consisting of heparin-proteoglycan. The network is produced by a protein and Ca^{++} binding to the sulphate groups of the proteoglycans, which implies a considerably larger concentration of free Ca^{++} ions in the lumen than in the cytosol. Now, the following reactions are running.

(i) Ca^{++} ions flow into the cytosol, the lumen Ca^{++} concentration decreases. (ii) When the corresponding concentration in the cytosol becomes too high the $InsP_3$ channel closes and the ASK_{Ca} opens. Sínce K^+ is present in the cytosol at higher concentration than in the vesicle lumen these ions diffuse into the lumen. (iii) At that point the crosslinked matrix in the vesicle comes into play. The monovalent K^+ partially replaces by ion-exchange the bound Ca and releases free Ca^{++} ions. (iv) Meanwhile the Ca^{++} concentration in the cytosol has decreased by diffusion to its originally low value. The $InsP_3$ channel opens again and the ASK_{Ca} channel closes. A new cycle starts with a cycle rate of 0.12 Hz. In principle this process could continue until equal K^+ ions are present in the lumen and the cytosol.

Later in his studies Verdugo and his team[29e] also realized that the flow of H^+ ions and the ion exchange K^+/H^+ had to be taken into account. Ca^{++} and H^+ concentration oscillations were found in phase. The interest of the biophysicists in this fact was focused on the signal broadcasting, which in this case would be required for reactions where both Ca^{++} and H^+ ions are needed. In addition we have to keep in

mind that with the exchange of Ca^{++} by K^{+} ions in the matrix, cross-links are broken. As a consequence the network swells stepwise with the periodic influx of K^{+} ions. The loss of Ca from the network continues to reach critical point where it goes through a phase transition undergoing a large change in volume that, of course, breaks the vesicle membrane. The expanded heparin network-this time without the membrane-can be easily recondensed by exposing it to conditions that mimic the intra-lumen conditions of the network.[30]

Scaffolds[31]

The terms ''scaffolding'' or ''tissue engineering'' are largely used interchangeably and refer to the preparation of materials that allow/encourage the growth of embedded cells into a three-dimensional structure. For polymer scientists this field of research offers a challenge of immense complexity. A few prerequisites may illustrate the difficulties. Clearly the (i) scaffolds have to be *biocompatible* with the cells or the native tissue, (ii) if at all possible, the artificial scaffold should be *degradable* by the native body when no longer needed, (iii) the scaffold should leave *pores for cells* to grow, and, (iv) it should be adaptable, but not rigidly so, in their response to the native body to allow *stable frames around the pores* but to prevent collapse. Figure 14 shows the range of tensile strength of several native tissues and the scale of elongation before break.

In the past much effort has been invested in the preparation of special microgels, e.g. as carriers for drugs of low water-solubility. The possibility of effective loading with drugs affords the preparation of a defined heterogeneity for binding the drug, but also the creation of small pores in the size of nanometers. However, in scaffolds pores have to be in the micro-scale i.e. *100 to 1000 times larger than for drugs*. This requirement offers the main challenge.

An examination of native extra-cellular networks gives a hint as to how the requirement of high tensile strength, combined with a mesh of micrometers in size, can be realized. In the fibrin network of blood clots the filaments of the net consist of side-by side aggregated double stranded fibrin chains. These double strands, initially formed, already have remarkable chain stiffness, a stiffness which is considerably enhanced within bundles of several such strands. Still the network retains remarkable elasticity by bending deformations at the crosslinks.[32] A similar principle is observed with the connective tissue from skin.[33] Here three structural elements of different properties come together. The high tensile strength is caused by a net of collagen fibres which can be very thick but in skin are thin and particularly smooth. This network furnishes the high tensile strength, but it still can be deformed at the crosslinks which may be considered as hinges. A collapse of the meshes is prevented by the osmotic pressure of

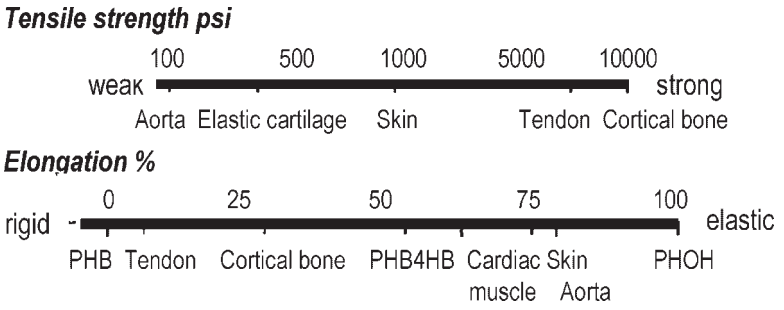

Figure 14.
Variation of tensile strength in selected native tissues and the corresponding elongation of break.(Redrawn after[31])

proteoglycans. These elements consist of a protein backbone with a number of grafted sulphated polysaccharide chains. The counter-ions of these highly charged sulphated chains establish a high osmotic pressure. The third component is hyaluran, a long, weakly charged anionic polysaccharide chain that mediates important interactions with the two other components to establish a reversible network.

The first attempts of preparing artificial scaffolds was made with bio-macromolecules, mainly polysaccharides. Good results were obtained with chitosan[34] and genetically modified alginates.[35,36] These materials are biodegradable but not always by enzymes from the human body.

Recently, promising suggestions have been made with synthetic poly(oxyalkonates).[37,38] Figure 15 shows the general chemical formula and a photograph from a scaffold prepared with poly(4-hydroxybutyrate), $M_w = 500\,000$ g/mol. The porous structure was obtained by a phase separation technique. A 5% solution of the polymer in dioxane was prepared at 60 °C. The solution was rapidly cooled to 0 °C in a suitable mould.

Around 11 °C dioxane froze, and simultaneously the polymer partially crystallized around the frozen dioxane domains. After evaporation the dioxane the porous structure of Figure 15 was obtained.[37]

Another polymer type with promising properties is offered by poly(phosphazenes).[39] Scheme 4 shows the general chemical formula. The polymers are biocompatible with human tissue and readily biodegradable. Interest arose from the behaviour of linear and slightly branched poly(alkylene oxides) as shown in the Table. These polymers are thermal sensitive and show lower critical solution temperatures (LCST) which implies tuning of the properties around body temperature from a swollen to a shrunken or collapsed structure.Reversible gelation can be achieved by Ca^{++} ions when the two residues of the monomer unit carry two acidic groups. When the crosslinking Ca^{++} ions are exchanged by K^+ ions, the network breaks down, and the system becomes soluble. It was speculated that by using asymmetric residues, e.g. side chains of $R_1 > R_2$ a reversible vesicle could be obtained.[39]

As a last example the work by Larreta-Garde eand co-worker[40] may be mentioned. In collaboration with Professor Djabourov she prepared a physical-chemical network by crosslinking gelatin via glutamyl-lysine crosslinks by adding transglutaminase at 40 °C and immediate

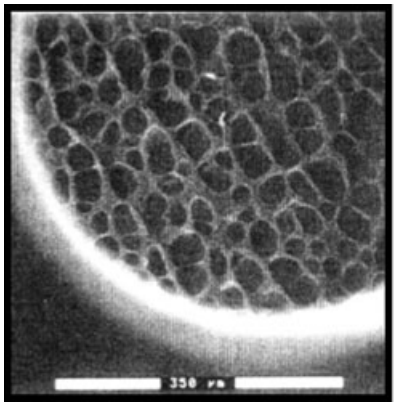

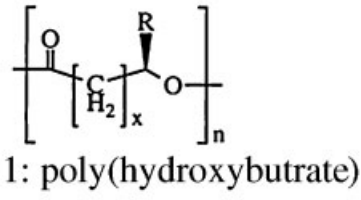

Figure 15.
Chemical structure of poly(oxyalkonates) and a photograph of a scaffold prepared from poly(4-hydroxybutyrate) (P4HB) using frozen dioxane drops as intermediate products. The porous structure was obtained after dioxane evaporation.[37] (By permission of Hartcourt Inc.)

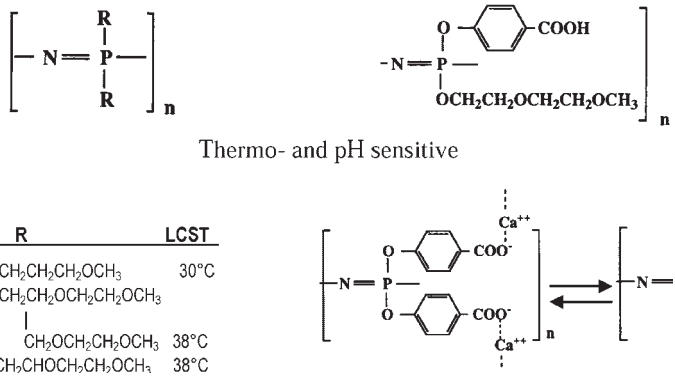

Scheme 4.
General chemical formula of poly(phophazenes) and of several thermally and pH sensitive derivatives (see Table). Of particular interest is the Ca^{++} sensitivity of the carboxyphenyl derivatives.[39] (By permission of Hartcourt Inc.)

cooling the system to 27 °C. Triple-helix formation and chemical crosslinking occurred simultaneously, but with a higher rate for the physical gelation, due to triple helix formation, than for the chemical reaction. The system resembles much the blood clotting process in which the physical gel stabilization of the clot is caused via glutamyl-lysine linkages between the dangling α-chain of the fibrin monomers. Then the physical-chemical network was submitted to a degradation reaction by adding a protease to the system, a process that again mimics the remove of the fibrin scaffold in nature.

This last example elucidates how close tissue engineering has come to the previously mentioned requirement that a biocompatible scaffold, that is needed for the growth of cells, should, in turn, be degradable when implanted in the body.

Acknowledgements: I wish to thank Professor Gert Heinrich, Polymer Institute Dresden, Dr. Annette Schmidt, University of Düsseldorf and Professor Walter Richtering, Technical University of Aachen for kindly providing me with their original data. I am grateful to my friends and colleagues for discussions and helpful comments in particular to Professor Simon Ross-Murphy, Kings College of London for his encouraging support of this contribution, in an area that was partly outside my own experience.

Books and Reviews on Polymer Networks

[1] A.H. Clark and S.B. Ross-Murphy Structural and Mechanical Properties of Biopolymers *Adv. Polym. Sci* **1987**, *83*, 60–191.
[2] J.E. Mark and B. Erman, Rubberlike Elasticity, Wiley, New York 1988.
[3] J.-M. Guenet Thermoreversible Gelation of Polymers and Biopolymers, Academic Press, London 1992.
[4] K. te Nijenhuis Thermoreversible Networks, *Adv. Polym. Sci.* **1997**, *139*, 1–252.
[5] R.F.T. Stepto (Editor) Polymer Networks, Principles of their Formation, Structure and Properties Blackie Academic & Profession, London 1999.
[6] P.A. Lovell, R.F.T. Stepto, A.N. Wilkinson (Eds) ''Professor J.L. Stanford. A celebration''. *Macromol. Sci., Part B: Physics* **2005**, *4*.

[1] See, for example, refs 1,3 and 4 above.
[2] [2a] D. A. Rees, *Adv. Carbohydr. Chem. Biochem.* **1969**, *24*, 26; *Biochem. J.* **1972**, *126*, 257; [2b] O. Smidsrod, A. Haug, *Acta Chem. Scand.* **1972**, *26*, 2063.
[3] [3a] E. van den Bosch, Q. Keil, G. Filipscei, H. Berghmans, H. Reynaers, *Macromolecules*, **2004**, *37*, 9673; [3b] J. de Rudder, H. Berghmans, F. C. de Schryver, M. Bocco, S. Paoletti, *Macromolecules* **2002**, *35*, 9529; [3c] J. de Rudder, H. Berghmans, P.

Adriaensens, D. Vanderzande, J. Gelan, S. Paoletti, *Macromolecules* **2001**, *34*, 522.
[4] [4a] H. J. Smallwood, *J. Appl. Phys.* **1944**, *15*, 758; [4b] A. Einstein, *Ann. Phys.* **1911**, *34*, 591.
[5] B. U. Felderhof, P. L. Iske, *Phys. Rev- A* **1992**, *45*, 611.
[6] R. B. Jones, R. Schmitz, *Physica A* **1983**, *122*, 105.
[7] J. Beriot, H. Montes, F. Leqzuex, D. Long, P. Sotta, *Macromolecules* **2002**, *35*, 9736.
[8] H. Montes, F. Lequeux, J. Beriot, *Macromolecules* **2003**, *36*, 8107.
[9] [9a] G. Huber, T. A. Vilgis, *Macromolecules* **2002**, *35*, 9104; [9b] G. Heinrich, M. Klüppel, T. Vilgis, Reinforcement Theories, in: J.E. Mark, *Physical Properties of Polymer Handbook*, Chap. 23. **2007**, in press.
[10] S. Westermann, M. Kreibelmann, W. Pickout-Hintzen, D. Richter, E. Straube, B. Farago, G. Goerigk, *Macromolecules* **1999**, *37*, 5793.
[11] G. Heinrich, E. Straube, G. Helmis, *Adv. Polym. Sci.* **1988**, *85*, 33.
[12] S. F. Edwards, T. A. Vilgis, *Rep. Prog. Phys.* **1988**, *51*, 243.
[13] M. Klüppel, J. Meier, G. Heinrich, Impact of pre-strain on dynamic-mechanical properties of carbon black and silica filled rubbers, in: *Constitutive models for Rubber III*, Bishfield, Muhr, Eds., Swets & Zeitlinger, **2006**.
[14] M. Klüppel, *Adv. Polym. Sci.* **2003**, *164*, 1.
[15] M. Klüppel, J. Schramm, *Macromol. Theor. Simul.* **2000**, *9*, 743.
[16] G. Heinrich, M. Klüppel, A. L. Svislov, Kautschuk, Gummi, K. G. K. Kunststoffe, **2005**, *58*, 163.
[17] J. L. Stanford, in: R. F. T. Stepto, Eds., "*Principles of theor Function, Structure and Properties*", Blackie Academic & Profession, London **1998**, Chapt 5, page 125.
[18] [18a] D. Nerger, Ph. D. Thesis, University of Freiburg 1978.[18b] M. Schmidt, W. Burchard, D. Nerger, *Polymer* **1979**, *20*, 582.
[19] [19a] V. Trappe, W. Burchard, *Local dynamics in branched polymers in: Light scattering and Photon spectroscopy*, E. R. Pike, J. B. Abbiss, Eds., Klüvers Acad. Publ. Dortrechtp **1997**, p. 142. [19b] V. Trappe, J. Bauer, M. Weissmüller, W. Burchard, *Macromolecules*, **1997**, *30*, 2365.
[20] W. Burchard, *Polym. Bull.* **2006**, published online, in print.
[21] W. Boyko, S. Richter, W. Burchard, Arndt, Langmuir online Nov. **2006**, in print.
[22] R. Pelton, *Adv. Colloid Interface Sci.* **2000**, *85*, 1.
[23] [23a] I. Berndt, J. S. Pedersen, W. Richtering, *J. Am. Chem. Soc.* **2005**, *127*, 9327; [23b] *Angew Chem. Int. Ed.* **2006**, *45*, 1. [23c] I. Berndt, W. Richtering, *Macromolecules* **2003**, *36*, 8780.
[24] D. Kunz, W. Burchard, *Colloid Polym. Sci. 264*, **1986**, p. 498.
[25] [25a] A. Kaiser, T. Gelbrich, A. M. Schmidt, *J. Phys, Cond. Matter* **2006**, special issue Ferrofluids; T. Gelbrich, M. Feyeen, A. M. Schmidt, *Macromolecules* **2006**, *39*, 3469. [25b] T. Gelbrich, M. Feyen, A. M. Schmidt, *Z. Phys. Chemie* **2006**, *220*, 41.
[26] A. M. Schmidt, *Macromol. Chem. Rapid Comun.* **2006**, *27*, 1168.
[27] A. J. Ryan, et al. *Macromol. Sci. Part B. Phys.* **2005**, *44*, 1103.
[28] See, autocatalysis and oscillating reactions in: P. W. Atkins, *Physical Chemistry*, Oxford University Press, Oxford **1994**.
[29] [29a] I. Nguyen, C. Wie-Chun, P. Verdugo, *Nature* **1998**, *395*, 908; [29b] I. Quesada, C. Wei-Chun, J. Steed, P-. Campos-Bedolla, P. Verdugo, *Biophys. J-* **2001**, *80*, 2133; [29c] I. Quesada, C. Wei-Chun, P. Verdugo, *Biophys. J.* **2003**, *85*, 963; [29d] I. Quesada, P. Verdugo, *Biophys. J.* **2005**, *88*, 3946; [29e] I. Quesada, C. Wei-Chun, P. Verdugo, *FEBS Lett.* **2006**, *580*, 2201.
[30] J. M. Fernandez, M. Villadon, P. Verdugp, J. Biophys, **1991**, *59*, 1022.
[31] A. Ataka, R. P. Lanza, Eds., *Methods of Tissue Engineering*, Academic Press, New York **2002**, Chapts. 42–64.
[32] M. W. Mosesson, R.F. Doolittle, Eds., *Molecular Biology of Fibrinogen and Fibrin* in particular; [32a] H. A. Scheraga, *Ann-. N. Y. Acad. Sci.* **1983**, *408*, 330; [32b] R. Hangen, J. McDonald, J. Hermans, *Ann. N. Y. Acad, Sci.* **1983**, *408*, 344.
[33] B. Alberts, A. Johnson, J. Lewis, M. Raff, K. Roberts, P. Walter, *Molecular Biology of the Cell*, Garland Science, 1091–1103 Fig. 19–41.
[34] C. D. Brown, A. S. Hoffmann, Chitosan, in: A. Ataka, R. P. Lanza, Eds., *Methods of Tissue, Engineering*, Academic Press, New York **2002**, Chapt. 47.
[35] K. H. Bouhadir, D. J. Mooney, Alginate Hydrogels.
[36] I. Donath, S. Holtan, Y. A. Murch, M. Dentini, G. Skjeak-Brak, *Biomacromolecules* **2005**, *6*, 1031.
[37] D. P. Martin, S. F. William, F. A. Skraly, Poly(hydroxyalkonates) in: A. Ataka, R. P. Lanza, Eds., *Methods of Tissue Engineering*, Academic Press. New York **2002**, Chapt. 48.
[38] A. Ataka, R. P. Lanza, Eds., *Methods of Tissue Engineering*, Academic Press, New York **2002**, Chapt. 56.
[39] H. R. Allock, Polyphosphazenes, in: A. Ataka, R. P. Lanza, Eds., *Methods of Tissue Engineering*, Academic Press, New York **2002**, Chapt. 51.
[40] S. Giraudier, V. Larreta-Garde, *Biomacromolecules* **2004**, *5*, 1662.

